PON Monitoring: Periodic Encoders With Low Capital and Operational Cost

Habib Fathallah, *Member, IEEE*, Mohammad M. Rad, *Student Member, IEEE*, and Leslie A. Rusch, *Senior Member, IEEE*

***Abstract*—We propose a novel and simple coding device for centralized monitoring of passive optical networks. Encoders have dual Bragg gratings forming a cavity producing periodic codes. These encoders reduce the cost of manufacturing, installation, inventory, and operation, while maintaining good performance and high capacity. We evaluate monitoring efficiency in terms of signal-to-noise ratio.**

***Index Terms*—Monitoring, network management, optical code-division multiplexing (OCDM), optical coding, passive optical network (PON), signal-to-noise ratio (SNR).**

I. Introduction

IN-SERVICE monitoring of time-division-multiplexed passive optical networks (PONs) is a serious open question. Some service providers report that more than 80% of installed PON failures occurs within the first/last mile, i.e., within the distribution/drop segments of the network. When a fault occurs, technicians must be dispatched to identify, locate, and fix the failure. The time, labor, and truck-roll for a fault identification dramatically increase the operational expenditure (OPEX) and erode profit margin. Furthermore, long repair time causes customer dissatisfaction and complaints. Therefore, a centralized monitoring, i.e., from the central office (CO) is highly desired because it provides instantaneous, full in-service information and control for service providers [1]–[5].

It is well known that optical-time-domain reflectometry (OTDR) is efficient for testing optical devices and monitoring of point-to-point networks; however, it is not effective for point-to-multipoint (PMP) networks like PONs [1]–[3]. In PMP networks, the OTDR trace at the CO is a linear sum of the backscattered and reflected powers from all network branches. It is difficult for the CO network manager to distinguish events in one branch from those in others. Chief among these problems is the difficulty to identify a specific broken branch in the PON tree architecture.

Few solutions exist for the monitoring of a PON. While imposing significant technical challenges, most techniques are impractical due to their limited capacity (tens of customers) [2]–[5]. In [6], we introduced, for the first time, a modified optical code-division-multiplexing (OCDM) scheme for centralized monitoring of PONs that is architecture agnostic. In this system, no active component is placed in the field and no intelligent module is embedded inside the customer's optical network terminal (ONT). In [7], we analyzed the performance of our monitoring system considering different encoder/decoder structures. In all our previous studies, we only considered standard coding schemes inspired from standard OCDM data communication. To our knowledge, despite their simplicity, the periodic codes (PCs) defined in this letter were never reported for standard direct sequence OCDMA.

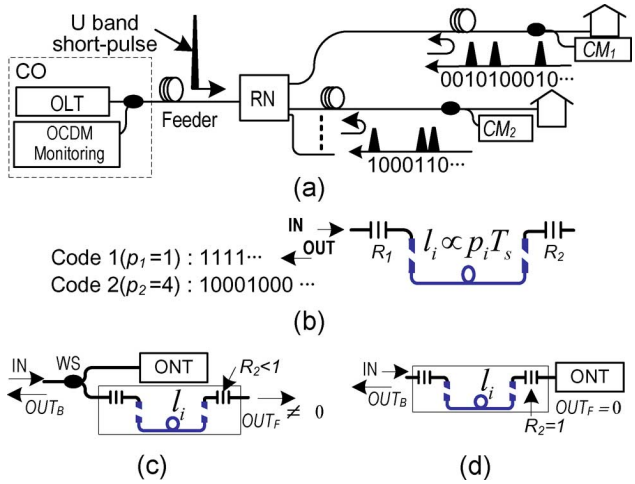

Fig. 1. (a) Optical coding monitoring system, (b) proposed CM structure, and two CM solutions (c) and (d).

In this letter, we propose a new coding scheme which is well adapted to the monitoring application. Our proposal reduces the overall cost of the monitoring system by developing simpler and lower cost optical coding devices. Recall that the PON market is very cost-sensitive, particularly for network elements not shared between customers, i.e., ONTs, distribution and drop fibers (DDFs), and passive coding devices for monitoring of each DDF. Our results show that our new proposal supports the monitoring of a 64 customer PON with signal-to-noise ratio (SNR) $\geq$ 10 dB.

A. Optical Coding Monitoring System

As illustrated in Fig. 1(a), a U-band short pulse with peak power P_s and duration T_s is transmitted through the feeder, split into N subpulses at the remote node, each of which is encoded and reflected back to the CO by a dual function device: encoder and mirror, we refer to as coding mirror (CM$_i$, $i = 1, \ldots, N$). Each DDF drop is terminated by a CM with a unique code, and is located physically close to the ONT. Information on individual

Manuscript received June 06, 2008; revised August 29, 2008. First published October 31, 2008; current version published December 12, 2008.

The authors are with Electrical and Computer Engineering Department, COPL, Universite Laval, Quebec, QC G1V0A6, Canada (e-mail: fhabib@gel.ulaval.ca; mohammad.mansouri-rad.1@ulaval.ca; rusch@gel.ulaval.ca; larusch@gelulaval.ca).

Color versions of one or more of the figures in this letter are available online at http://ieeexplore.ieee.org.

Digital Object Identifier 10.1109/LPT.2008.2006060

DDFs is discernable at the CO due to the near orthogonality of the codes. The CO monitoring equipment decodes the received signal for the target line; a healthy target DDF contributes an autocorrelation peak, while nontargeted DDFs contribute cross-correlation spikes.

In [6] and [7], we considered the CO monitoring equipment with a programmable decoder that correlates the received signal cyclically for each subscriber line. The correlated (or decoded) signal is then photodetected, and the autocorrelation peak is identified by an electric threshold that rejects cross-correlation spikes and noise. In this letter, however, we propose the decoding functions be implemented in electronics after the photodetector. Our PON monitoring system exploits short pulses (subnanosecond to a few nanoseconds). The gigahertz speed electronics required are economically feasible today, especially for the CO equipment whose cost can be amortized over the client base. In addition to reducing the cost of the monitoring system, electronic decoding eliminates the power insertion and decoding loss, hence alleviating the loss/power budget of the system. Furthermore, electronic decoding reduces substantially the so-called beat noise that limits performance of OCDM systems. Our analysis of SNR captures the increase in power budget, but does not reflect the further improvement when reducing beat noise.

B. CMs Based on Optical Cavity

All previously proposed CMs are composed of high loss passive splitters or a series of Bragg gratings as in standard OCDM systems [6]. These schemes require a wavelength selector (WS) multiplexing/demultiplexing the U-band from data bands at the CO and DDF terminations. Moreover, Bragg gratings CMs require one grating for every pulse (or logical 1) in the code; the relative distances between gratings in the fiber differ from one code to another depending on the positions of ones in the code. The high number of components and their assembly increase the manufacturing, installation, and inventory cost. For instance, a coding device that is composed of many gratings, each of which has its own power reflectivity and physical placement in the fiber, involves high manufacturing, splicing, and packaging complexity, increasing the cost of the installation, repair, and inventory.

In this letter, we propose a new simple coding structure that exploits only two Bragg gratings written for the same wavelength and forming an optical cavity [see Fig. 1(b)]. A single incident pulse generates an infinite sequence of equally spaced multilevel pulses in reflection. We further suppose that each subscriber has a pair of Bragg gratings with the same reflectivities R_1 and R_2, and the same center wavelength. Only a unique physical separation l_i of the grating distinguishes one subscriber from the next, i.e., each subscriber has a unique cavity length. We refer to the code generated by this cavity as a multilevel periodic code (ML-PC).

The grating power reflectivities R_1 and R_2 fix the levels of the reflected sequence of pulses; as these reflectivities are identical for all codes, the levels are identical for all codes. An ML-PC is thus determined by the length of the silent intervals separating the multilevel pulses, i.e., its period. The period of the ith code is unique and related to the cavity length l_i by

$$p_i = 2\frac{nl_i}{cT_s}, \qquad i = 1, \ldots, N \tag{1}$$

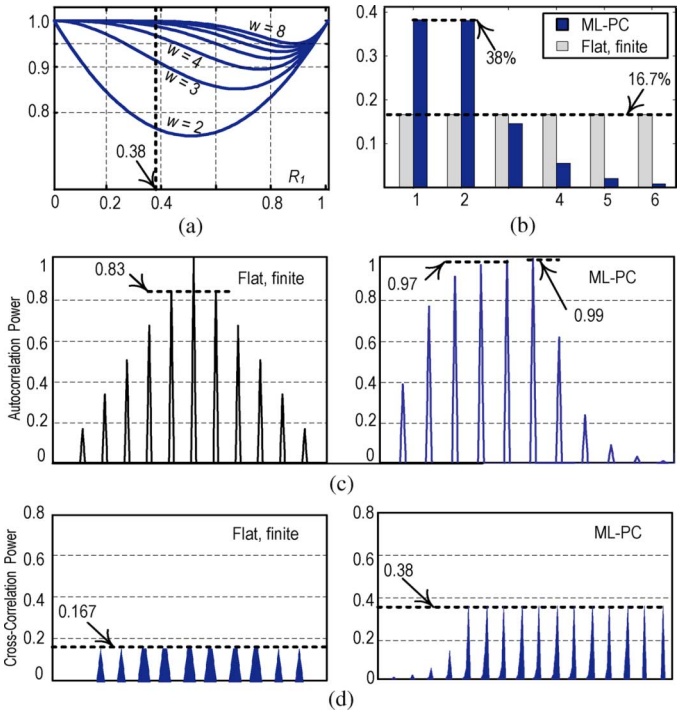

Fig. 2. Example of a flat, finite code and an ML-PC code. (a) Total decoded power ML-PC; (b) flat versus ML-PC code; (c) normalized autocorrelation for $p_3 = 9$ and $w = 6$; (d) normalized cross-correlation for $p_3 = 9$ and $p_6 = 17$, $w = 6$.

given in units of pulse duration, where n is the effective group index and c is the speed of light in the fiber core. The fiber length inserted between gratings fixes cavity length and differentiates the codes. In Fig. 1(b), we show a logical description of PCs for $p_1 = 1$ and $p_2 = 4$. When $T_s = 1$ ns, l_1 and l_2 equal 10 and 40 cm, respectively.

Fig. 1(c) and (d) illustrates two solutions for our cavity-based CM. The first allows R_2 to be inferior to one, so the incident pulse power can be split between backward (OUT_B) and forward (OUT_F) paths. This scheme allows greater flexibility in using R_1 and R_2 to fix code pulse levels; however, insertion loss is nonnegligible and a WS is required [6]. The second solution fixes $R_2 = 1$, constraining all power to be reflected back to the CO (i.e., $\mathrm{OUT}_F = 0$). This reduces CM cost as no WS is needed, and improves power budget. In the following, we focus on the latter scheme.

C. CM Design

Recall that R_1 and R_2 determine the levels of the code pulses when neglecting cavity length induced loss. When R_2 is fixed to one, only R_1 dictates these levels. Let ρ_j be the height (or level) of the jth pulse generated by the cavity. We find ρ_j from

$$\rho_j = \begin{cases} R_1, & j = 1 \\ (1 - R_1)^2 R_1^{j-2}, & j \geq 2. \end{cases} \tag{2}$$

As an optimization criterion, we seek to concentrate reflected power in a few pulses. This avoids long codes with greater interference between codes. Fig. 2(a) illustrates the total power contained in the first w pulses of the sequence as a function of R_1. The ML-PC code (dark bars) illustrated in Fig. 2(b) corresponds to $w = 6$ and $R_1 = 0.38$, ensuring 99% of the incident pulse power is reflected in the first six pulses.

The simple structure of our PCs enables us to produce any desired number of codes no matter constraints on code weight and correlation. We developed a simple algorithm for determining the codes:

1) Knowing the desired code weight w, we obtain the first code corresponding to a period $p_1 = 1$.
2) The ith code has period $p_i = p_{i-1} + 1$ if its maximum cross-correlation with all the kth codes $(k = 1, \ldots, i-1)$ is one, otherwise increment p_i until meeting this constraint.

D. ML-PC Code Properties

ML-PC codes have infinite length, but pulse heights die out exponentially. We assume the receiver has perfect knowledge of the observation window at the autocorrelation peak, i.e., the exact location of the desired customer in the network. We consider ML-PC codes with power concentrated into a small number of w pulses. Fig. 2(b) shows a truncated version of an ML-PC (dark bars); the first $w = 6$ pulses contain 99% of the total code power. For simplicity, we always normalize the total code power to one. We also assume the decoder correlates the received signal with the truncated version of the code, $w = 6$ being the weight of the decoder. In Fig. 2(b), for comparison with the ML-PC code (dark bars) we also consider a flat, finite, weight 6 code (gray bars). Note the flat, finite code is not achievable with our cavity encoder.

The autocorrelation function for code $p_3 = 9$ for both ML-PC and flat infinite codes is given in Fig. 2(c). We observe a main lobe of one for flat finite codes (the sum of six equal pulses), and 0.99 for ML-PC (the sum of its six unequal pulses). We see high out-of-phase sidelobes with a maximum at the superposition of $w - 1$ pulses (similar to prime codes). For flat finite PC $(w - 1/w) = (5/6) = 0.83$, however, for ML-PC this is 0.97 (the sum of its highest five pulses). High autocorrelation sidelobes are not problematic as pulses are separated by more than the sidelobe durations. In the case of cross-correlation, by design, only one high sidelobe could possibly fall in the observation window, however, lower sidelobes would be desirable. The cross-correlation examples in Fig. 2(d) consider codes with periods $p_3 = 9$ and $p_6 = 17$. We obtain unitary cross-correlation, i.e., $(1/6) = 0.167$ for flat finite codes and 0.38 for ML-PC.

II. Performance Evaluation

In order to assess the performance of this monitoring technique with the proposed multilevel codes, we consider the following expression for the SNR:

$$\mathrm{SNR} \triangleq \frac{\mu_{\mathrm{SIG}}^2}{\sigma_N^2} = \frac{\mu_{\mathrm{SIG}}^2}{\sigma_{\mathrm{TH}}^2 + \sigma_{\mathrm{D}}^2 + \sigma_{\mathrm{SH}}^2 + \sigma_{\mathrm{BN}}^2} \tag{3}$$

where μ_{SIG} and σ_N^2 are, respectively, the useful signal and total noise power in the autocorrelation main lobe. Index TH is used for thermal noise (spectral density 0.1 pA $\cdot$ Hz$^{-0.5}$), D for dark current (average current 160 nA), SH for shot noise, and BN for beat noise (this include the interference noise). A coherent laser source at $\lambda = 1650$ nm corresponding to 0.3-dB/km fiber loss is assumed. We also considered $T_s = 1$ ns and $P_s = 4$ dBm. To compensate the system loss, we use an avalanche photodiode with gain of 100 and excess noise factor of 7.9. We considered an aggregate excess loss of 5 dB for splicing, connectors, etc. The clients are considered to be uniformly distributed over 1-km^2 coverage area after a 20-km feeder [7]. Fig. 3 illustrates the SNR as a function of the number of customers. For a 64 customer PON, the proposed ML-PCs achieve 10.6-dB SNR; this represents less than 1-dB penalty compared to the binary, flat, finite code. Negligible difference exists between binary and ML-PCs. This result is intuitively true because for the ML-PC the autocorrelation main lobe includes 0.99 of the desired power compared to the binary codes.

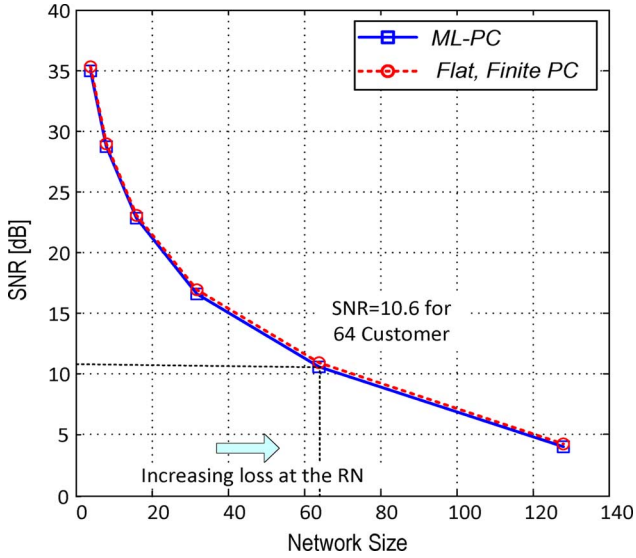

Fig. 3. SNR of binary versus ML-PC.

III. Conclusion

We proposed and analyzed a new optical coding device that trades suboptimum performance in high-capacity PONs for reducing the capital (CAPEX) and operating (OPEX) expenses of PON monitoring system. An SNR of 10 dB is achieved for a 64 customer PON with households randomly distributed over the 1-km^2 coverage area.

References

[1] A. Girard, *FTTx PON Technology and Testing*. Canada: EXFO Electro-Optical Engineering Inc., 2005, ISBN 1-55342-006-3.
[2] D. Iida, N. Honda, H. Izumita, and F. Ito, "Design of identification fibers with individually assigned Brillouin frequency shifts for monitoring passive optical networks," *J. Lightw. Technol.*, vol. 25, no. 5, pp. 1290–1297, May 2007.
[3] S. Hann, "Monitoring technique for a hybrid PS/WDM-PON by using a tuneable OTDR and FBGs," *Meas. Sci. Technol.*, vol. 17, pp. 1070–1074, 2006.
[4] C. Yeh and S. Chi, "Optical fiber-fault surveillance for passive optical networks in S-band operation window," *Opt. Express*, vol. 13, no. 14, pp. 5494–5498, Jul. 2005.
[5] S. B. Park *et al.*, "Optical fault monitoring method using broadband light source in WDM-PON," *Electron. Lett.*, vol. 42, no. 4, pp. 239–241, Feb. 2006.
[6] H. Fathallah and L. A. Rusch, "Code-division multiplexing for in-service out-of-band monitoring of live FTTH-PONs," *J. Opt. Netw.*, vol. 6, no. 7, pp. 819–827, Jul. 2007.
[7] M. M. Rad, H. Fathallah, and L. A. Rusch, "Effect of PON geographical distribution on monitoring by optical coding," presented at the ECOC, Germany, Sep. 2007.
[8] M. M. Rad, H. Fathallah, and L. A. Rusch, "Beat noise mitigation via hybrid 1D/2D-OCDM: Application to monitoring of high capacity PONs," presented at the OFC, San Diego, CA, Feb. 2008, Paper OMR7.